agriculture

MDPI

Article

Calibration of Simulation Parameters for Fresh Tea Leaves Based on the Discrete Element Method

Dongdong Li [1], Rongyang Wang [2,*], Yingpeng Zhu [1], Jianneng Chen [1,*], Guofeng Zhang [1] and Chuanyu Wu [1]

[1] College of Mechanical Engineering, Zhejiang Sci-Tech University, Hangzhou 310018, China; 17816037677@163.com (D.L.); 201910501018@mails.zstu.edu.cn (Y.Z.); zhguof@zstu.edu.cn (G.Z.); cywu@zstu.edu.cn (C.W.)

[2] College of Intelligent Manufacturing and Elevator Technology, Huzhou Vocational and Technical College, Huzhou 313000, China

* Correspondence: rongyang1987@126.com (R.W.); jiannengchen@zstu.edu.cn (J.C.)

Abstract: To address the problem of a lack of accurate parameters in the discrete element simulation study of the machine-picked fresh tea leaf mechanized-sorting process, this study used machine-picked fresh tea leaves as the research object, established discrete element models of different fresh tea leaf components in EDEM software version 7.0.0. based on the bonded particle model using three-dimensional scanning inverse-modeling technology, and calibrated the simulation parameters through physical tests and virtual simulation tests. Firstly, the intrinsic parameters of machine-picked tea leaves were measured using physical tests; the physical-stacking tea leaf test was conducted using the cylinder lifting method, the tea leaf repose angle being 32.62° as measured from the stacking images using CAD. With the physical repose angle as the target value, the Plackeet–Burman test, the steepest-ascent test and the Box–Behnken optimization test were conducted in turn, and the results showed that the static friction coefficient between tea leaves, the rolling friction coefficient between tea leaves and the static friction coefficient between tea leaves and PVC have a major effect on the repose angle, and the optimal combination of the three significant parameters was determined. Finally, five simulations were conducted using the optimal combination of parameters, the relative error between the repose angle measured by the simulation test and the physical repose angle being just 0.28%. Moreover, the *t*-test obtained $p > 0.05$, indicating that there was no significant difference between the simulation test results and the physical test results. The results showed that the calibrated discrete element simulation parameters obtained could provide a reference for the discrete element simulation study of fresh tea leaves.

Keywords: fresh tea leaves; parameter calibration; repose angle; discrete element method; three-dimensional scanning

Citation: Li, D.; Wang, R.; Zhu, Y.; Chen, J.; Zhang, G.; Wu, C. Calibration of Simulation Parameters for Fresh Tea Leaves Based on the Discrete Element Method. *Agriculture* **2024**, *14*, 148. https://doi.org/10.3390/agriculture14010148

Academic Editor: Dainius Steponavičius

Received: 11 December 2023
Revised: 3 January 2024
Accepted: 17 January 2024
Published: 19 January 2024

1. Introduction

Tea is rich in polyphenols, proteins, amino acids, vitamins, and other nutrients, offers good health benefits and is one of the most important cash crops in China. By the end of 2022, the area under tea plantations in China had increased to nearly 50 million mu, and tea production has continued to increase steadily [1]. With the increasing scale of the tea industry and its increasing labor costs, the picking of fresh tea leaves has become an important factor limiting the industry's development. Consequently, mechanized picking has become an inevitable trend, with the current mechanized picking process being primarily a rigid, non-selective picking method, resulting in problems such as the uneven length, uneven age, and low uniformity of machine-picked fresh tea leaves [2]; this affects both the quality of finished tea and its economic benefits, making it necessary to sort the tea leaves to obtain different grades of tea leaves. In recent years, the discrete element method (DEM) has been widely used to study the kinematic behavior of bulk

materials in agriculture in terms of the interaction between the bulk material and the relevant machinery [3,4].

To improve the accuracy of discrete element simulation, it is necessary to accurately establish the discrete element model of the material and accurately define its intrinsic and contact parameters [5,6]. The intrinsic parameters are usually measured directly, using physical bench tests; the contact parameters of materials may be difficult to measure, resulting in inconsistent simulation and physical test results [7]. Consequently, the calibration of the intrinsic and contact parameters is required for the simulation tests of agricultural material models.

To date, many studies on the calibration of discrete element parameters have been conducted for different agricultural materials, including soil [8,9], grain seeds [10–12], crop straws [11,13–16], and fruit and vegetables [17,18], amongst others. Qiu et al. [9] used the Plackett–Burman design and response surface method to calibrate the discrete element simulation parameters of cinnamon soil based on the Hertz–Mindlin model with the JKR contact model. Hou et al. [10] established a discrete element model for Agropyron seed and calibrated the contact parameters using a combination of physical and simulation tests. Bart et al. [16] developed a bendable straw–stalk model to study the grain–straw separation process and conducted a sensitivity study on the mechanism influencing the crop characteristics and separation rate. Du et al. [17] used reverse engineering technology to build a discrete element model of pod pepper and calibrated its contact parameters using the response surface method. Ren et al. [19] constructed a discrete element model of sugarcane leaves using the multi-sphere aggregation method, and the contact parameters of sugarcane leaves were optimized and calibrated using the response surface method. Zhu et al. [20] used the DEM to calibrate the lunar soil simulant parameters to accurately simulate the interaction between the lunar rover wheels and the lunar soil simulant. Zhang et al. [21] established a single-root model of maize of different diameters and a maize-root–soil mixture model, the discrete element parameters of the maize-root–soil mixture being calibrated using the response surface method. Yu et al. [22] established a discrete element model of fresh Goji berries using the multi-spherical particle method, and calibrated the discrete element contact parameters using a combination of physical and simulation tests, the physical repose angle being the target value.

In this study, the intrinsic parameters of different components of fresh tea leaves are measured using physical tests, combined with three-dimensional scanning technology. A discrete element model of different components of fresh tea leaves based on the bonded particle model was developed; using a combination of physical and simulation tests, the physical repose angle of fresh tea leaves was used as the response value, and the DEM contact parameters of fresh tea leaves were calibrated using the design of the experimental method, to conduct simulation tests for verification purposes, and to provide reliable discrete element simulation parameters for the simulation of tea mechanization operations and equipment development—such as fresh tea leaf sorting.

2. Materials and Methods

2.1. Geometric Measurement of Fresh Tea Leaves

To accurately develop the fresh tea leaf discrete element model, this study selected "tea 108" from the Hangzhou Institute of Agricultural Science of Tea, with one hundred single buds, one bud and one leaf, and one bud and two leaves without insect damage or pathological characteristics being randomly selected from the tea garden. The leaf length (L) and width (W) were measured using digital display vernier calipers (accuracy of 0.1 mm), separately (as shown in Figure 1), and the leaf thickness was measured using a micrometer (as shown in Figure 2); the test was repeated 3 times, the measurements of which are shown in Table 1.

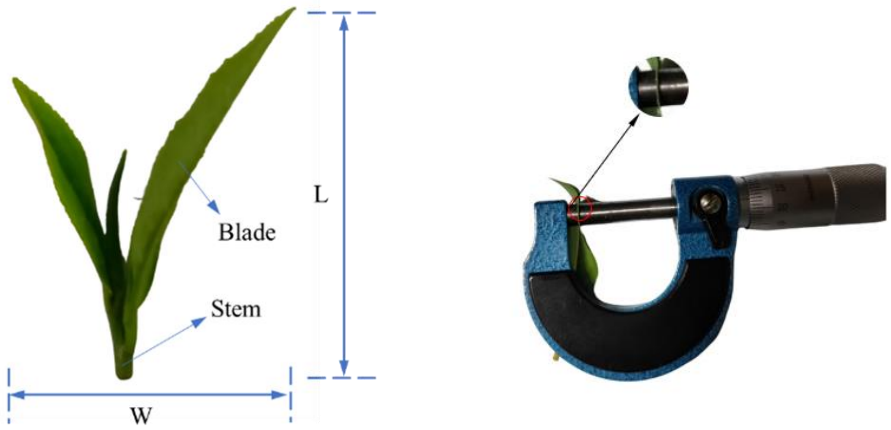

(**a**) (**b**)

Figure 1. Geometric dimensions of fresh tea leaves: (**a**) leaf length (L) and leaf width (W); (**b**) leaf thickness (T).

(**a**) (**b**)

Figure 2. Density measurement of fresh tea leaves: (**a**) quality measurement of tea leaves; (**b**) volume measurement of tea leaves.

Table 1. Shape parameters of fresh tea leaves.

Leaf Type	Leaf Length/mm	Leaf Width/mm	Leaf Thickness/mm
Single bud	15~25	3~6	0.15~0.17
One bud and one leaf	25~35	10~20	0.18~0.23
One bud and two leaves	35~60	20~40	0.24~0.30

According to the measured data, the average leaf length and leaf spreading of a single bud were 19.6 and 3.8 mm, respectively; the average leaf length and leaf spreading of one bud and one leaf were 29.5 and 13.8 mm, respectively; and the average leaf length and leaf spreading of one bud and two leaves were 45.2 and 29.3 mm, respectively. Among them, the thickness of the tea leaves is generally in the range of 0.15~0.3 mm.

2.2. Density Measurement of Fresh Tea Leaves

Fresh machine-picked tea leaves belong to bulk materials, and the density measured in this paper is the true density, the measurement standard being based on the measurement method of solid density in the GB/T4472-2011 standard [23]. First, an electronic balance with an accuracy of 0.01 g was used to weigh the fresh tea leaf mass (M) of 2~5 g, after which a measuring cylinder with an accuracy of 0.1 mL was used to measure the pure water

volume (V_0). The fresh tea leaves were completely immersed in the measuring cylinder using a glass rod, and the total volume (V_1) of water and fresh tea leaves in the measuring cylinder was recorded (as shown in Figure 2). The difference between the two values was the volume of fresh tea leaves. Based on the principle of solid density measurement, we could calculate the fresh tea leaf density using Equation (1), repeated 10 times to obtain an average value, the density of fresh tea leaves being 851.4 kg m^{-3}. The calculation as shown in Equation (1) is the following:

$$\rho = \frac{M}{V_1 - V_0} \tag{1}$$

where M denotes the mass of fresh tea leaves (kg), V_0 denotes the volume of water in the measuring cylinder without the addition of fresh tea leaves (m^3), V_1 denotes the total volume in the measuring cylinder after adding the fresh tea leaves, and ρ denotes the density of the fresh tea leaves (kg m^{-3}).

2.3. Modulus of Elasticity and Shear Modulus

The modulus of elasticity is one of the important parameters in discrete element simulation [24]. Since tea leaves are thin and soft materials, it is impossible to conduct compression tests on them, so their stems were cut into small circular segments of length 3 mm using a utility knife, and uniaxial compression tests were conducted using a TMS-PRO mass spectrometer (Zhuohao Laboratory Equipment Co., Ltd, Shanghai, China), as shown in Figure 3 [25]. During the test, the diameter of the stem segment was measured using a vernier caliper, after which the stem segment was placed vertically on the loading table of the mass spectrometer, and a 38.1 mm-diameter circular probe was used to set the compression speed to 10 mm/min and the loading displacement to 1 mm, the probe being automatically returned to its original position at the end of the test. The test was repeated 10 times, the average value of the elastic modulus of tea leaves being 9.24 MPa, the shear modulus being 3.3 MPa, and Poisson's ratio being 0.4 using Equation (2), Equation (3), and Equation (4), respectively. The calculation as shown in Equations (2)–(4) is the following:

$$E = \frac{F}{A \cdot \varepsilon} \tag{2}$$

$$G = \frac{E}{2(1+\mu)} \tag{3}$$

$$\mu = \frac{|\varepsilon_2|}{|\varepsilon_1|} = \frac{\Delta d l_0}{\Delta l d_0} \mu = \frac{|\varepsilon_2|}{|\varepsilon_1|} = \frac{\Delta d l_0}{\Delta l d_0} \tag{4}$$

where E is the modulus of elasticity (MPa), F is the axial load applied to the fresh leaf stem (N), A is the contact area (mm^2), ε is the strain, G is the shear modulus (MPa), μ is Poisson's ratio, l_0 is the pre-test length of the fresh leaf stem (mm), d_0 is the pre-test diameter of the fresh leaf stem (mm), Δl is the change in the length of the fresh leaf stem after the test, Δd is the change in diameter of the fresh leaf stem after the test (mm), ε_2 is the transverse strain, and ε_1 is the longitudinal strain.

2.4. Measurement of Physical Angle of Repose

The repose angle of fresh tea leaves is one of the more important indicators for characterizing the macroscopic properties of tea materials—including the flow properties and internal friction characteristics [26]. In this study, a bulk material stacking-angle measurement method was used to determine the actual repose angle of fresh tea leaves based on the JB/T9014.7-1999 standard [23], using the cylinder lifting method (Figure 4). The test sample was machine-picked fresh tea leaves; using a PVC hollow cylinder of inner diameter 100 mm and height 200 mm, after filling the cylinder with fresh tea leaves and then lifting the cylinder at a constant speed of 0.2 m/s, so that the tea leaves fall out of the cylinder naturally, a pile of tea fresh leaf materials forms on the horizontal bottom plate, and the angle between the bus bar and the horizontal plane of the accumulation is

measured. We repeated the above test 10 times to obtain an average value of the repose angle of fresh tea leaves, which was 32.62°.

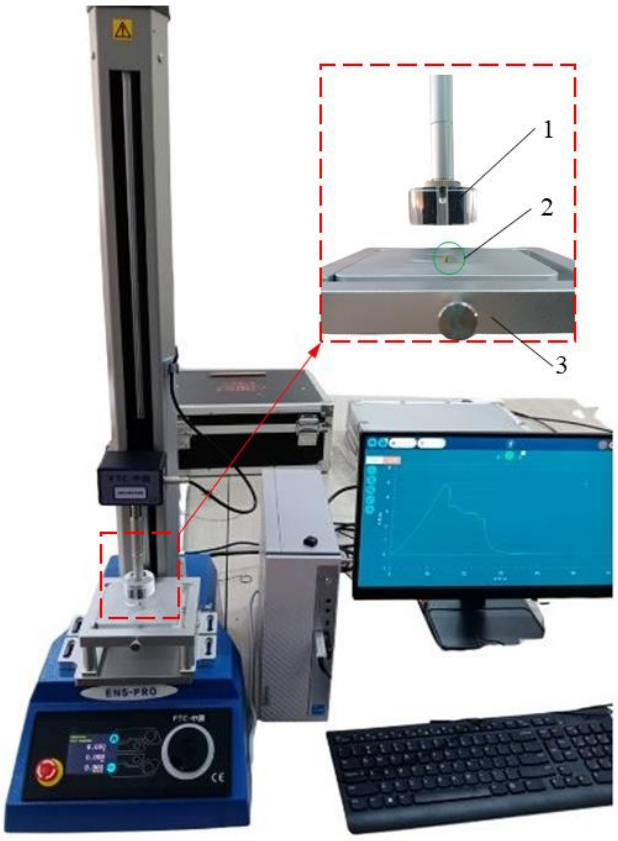

Figure 3. Mass Spectrometer. 1—compression probe, 2—fresh leaf stem, 3—carrier table.

Figure 4. Physical repose angle test of fresh tea leaves.

2.5. Discrete Element Model of Machine-Picked Fresh Tea Leaves Based on 3D Scanning

2.5.1. Contour Model

Owing to the irregular appearance of fresh tea leaves, conventional modeling methods cannot accurately restore their real characteristics. The aim is to establish more accurate 3D models of fresh tea leaves and improve the accuracy of simulation tests while also considering the limitations of non-spherical particle modeling using EDEM software version 7.0.0., to reduce the simulation time and calculation of overheads, as shown in Figure 5. Fresh tea leaves—namely, a single bud, one bud and one leaf, and one bud and two leaves—whose leaf length and leaf spreading were close to the average values were selected as the research object.

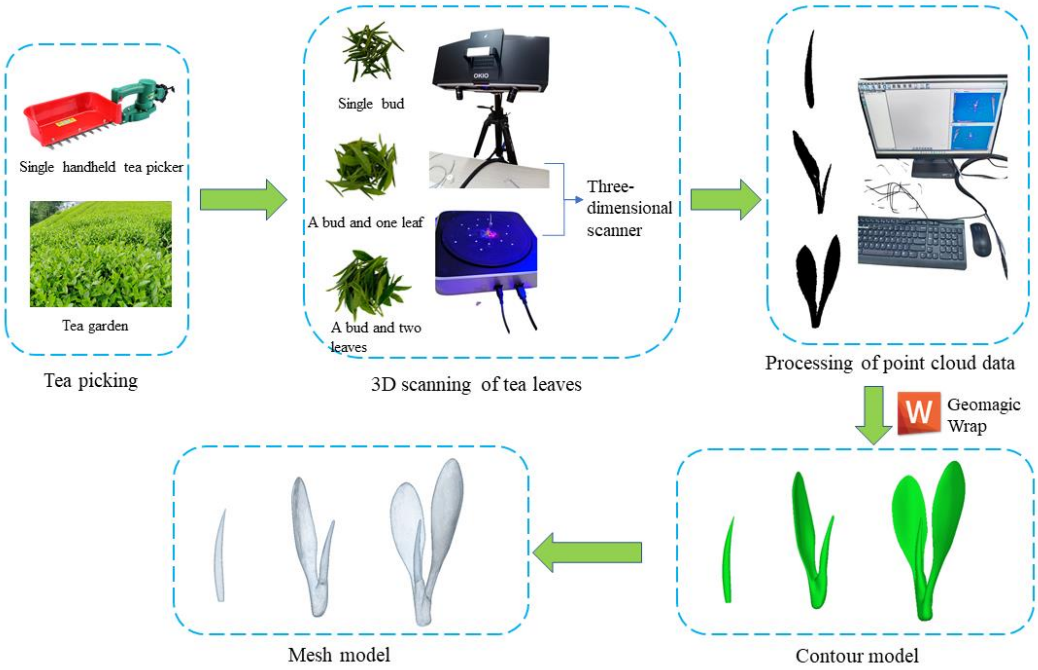

Figure 5. The acquisition process of a fresh tea leaf 3D model.

As is evident from Figure 5, the Tianyuan 3D OKIO scanner is used to scan the outer contour of the fresh tea leaves using blue light non-contact photography, to accurately obtain the three-dimensional coordinates of the outer surface of the tea leaves, and obtain their point cloud data. The point cloud data were then imported into Geomagic Wrap software version 2017 for inverse modeling, and the operations of coloring, noise reduction, point cloud triangulation, merging, smoothing and model correction were conducted in turn to obtain a 3D solid model. Finally, the solid model was imported into Hypermesh software version 2021 for meshing to obtain the tea mesh model.

2.5.2. Discrete Element Model

The tea leaf discrete element model adopts a multi-sphere bonded particle model comprising several spherical particles of equal diameter bonded by "Bond" to simulate the characteristics similar to those of real tea leaves. The smaller the radius of the spherical particles used, the larger the number of bonded spherical particles, and the smaller the radius of the spherical particles used, the closer they are to the tea leaves' profile model; however, the time cost of simulation greatly increases. The fresh tea leaf 3D contour model is imported into EDEM 2021 software as a geometry, and the spherical particle material is added, a spherical particle of radius 0.25 mm being used for filling, using the pre-filling test. After the filling is completed, the fresh tea leaf discrete element model can be obtained, as shown in Figure 6. In the EDEM post-processing interface, the radius size, ID number, and spherical center coordinate parameters of spherical particles are exported. According to statis, the number of filled particles of discrete element models of different components of fresh tea leaves—that is, the single bud, one bud and one leaf, and one bud and two leaves—are 284, 2286 and 4608, respectively.

Since tea leaves belong to flexible materials, they easily produce a certain degree of bending after collision in the process of movement. To improve the realism of fresh tea leaf simulations, it is necessary to build a flexible discrete element model and adopt the meta-particle model of Bonding V2. The contact radius of the discrete element multi-sphere model can be set to detect whether the particles are bonded, and when the contact radius of the spheres detects contact a "Bond" key is generated to bond the two spheres together. If the contact radius is too small, the bonding model is brittle, and if the contact radius is too large, a bond will be generated between non-contacting particles in the bonding model. To

reduce the effect of the contact radius on the simulation results, the contact radius should be 20–30% larger than the physical radius [23].

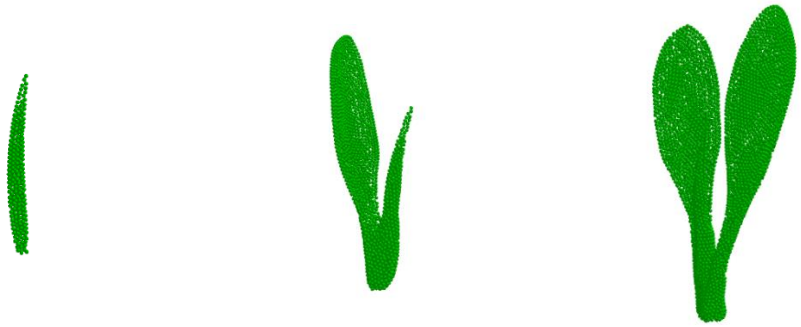

(**a**) (**b**) (**c**)

Figure 6. Discrete element model of fresh tea leaves: (**a**) single bud; (**b**) one bud and one leaf; (**c**) one bud and two leaves.

Based on the coordinate information of spherical particles filled with fresh tea leaves mentioned above, the physical radius of particles was set to 0.25 mm and the contact radius was set to 0.3 mm. Combined with the discrete element simulation parameters of fresh tea leaves and PVC in the literature [27,28], the range of discrete element simulation parameters in this study are as shown in Table 2. Based on the data obtained from the compression test, after calculation and multiple simulation adjustments, the Bonding parameters of the discrete elements of fresh tea leaves as set in Table 3 could be obtained, and a flexible bond model of discrete elements established (as shown in Figure 7).

Table 2. Parameters required in DEM simulation.

Parameter	Value
Poisson's ratio of tea leaves	0.4
Density of tea leaves (kg·m^{-3})	851.4
Shear modulus of tea leaves (Pa)	3.3×10^6
Poisson's ratio of PVC	0.45
Density of PVC (kg·m^{-3})	1200
Shear modulus of PVC (Pa)	1.8×10^{10}
Tea leaves–tea leaves restitution coefficient	0.01~0.09
Tea leaves–tea leaves static friction coefficient	0.8~1.0
Tea leaves–tea leaves rolling friction coefficient	0.01~0.2
Tea leaves–PVC restitution coefficient	0.01~0.2
Tea leaves–PVC static friction coefficient	0.6~0.8
Tea leaves–PVC rolling friction coefficient	0.01~0.05

Table 3. Bonding parameters of tea granules.

Bonded Parameter	Value
Normal stiffness coefficient (N·m^{-1})	5×10^9
Tangential stiffness coefficient (N·m^{-1})	3×10^9
Normal critical stress (MPa)	1.6×10^3
Shear critical stress (MPa)	1.2×10^3

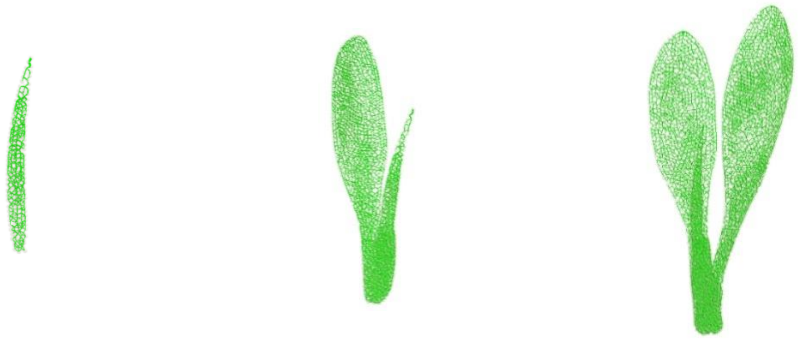

(**a**) (**b**) (**c**)

Figure 7. BondingV2 model of fresh tea leaves: (**a**) single bud (**b**) one bud and one leaf (**c**) one bud and two leaves.

2.6. DEM Simulation Test

In the EDEM 2021 software, a hollow cylinder (of inner diameter 100 mm and height 200 mm) was added, and a virtual plane created above the cylinder as a particle plant. The fresh tea leaf simulation stacking test is shown in Figure 8.

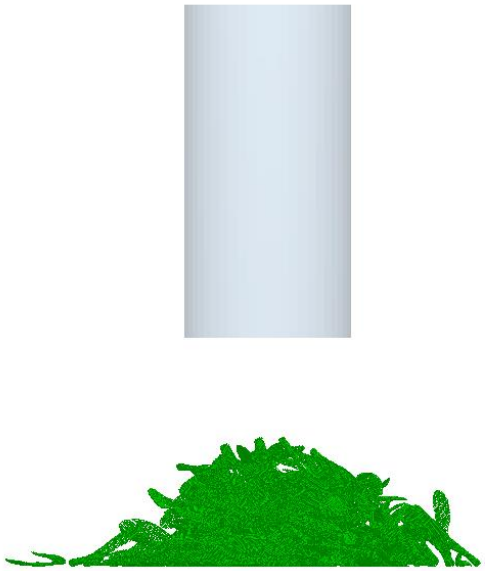

Figure 8. Simulation test of the repose angle.

The particle generation method is dynamic; the generation rates of the single bud, one bud and one leaf, and one bud and two leaves are set to 0.002, 0.018, and 0.035 kg s^{-1}, respectively, and the total generated fresh tea leaf mass is 55 g. The total simulation time is 3 s, and when the fresh tea leaf particles are stabilized, the hollow cylinder is lifted at a speed of 0.2 m s^{-1}, and the particles form a material pile when they are stationary on the plane.

Using Protractor, a built-in angle measurement tool in the software, the repose angle is measured in both the +X and +Y directions using the center of the stacked body as the measurement origin, and the results are averaged. The simulated repose-angle measurement diagram is shown in Figure 9.

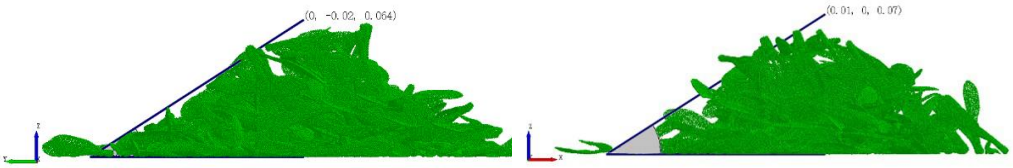

(**a**) (**b**)

Figure 9. Measurement of repose angle in simulation test: (**a**) tea leaf stacking +X direction, (**b**) tea leaf stacking +Y direction.

3. Results and Discussion

3.1. Analysis of the Simulation Results of the Plackett–Burman Test

The Plackett–Burman test was used to determine the significance of each factor by comparing the differences between the two levels of each factor based on the relationship between the target response and each factor, to quickly screen out the factors that had a significant effect on the response values [29]. In this study, the Plackett–Burman test design was conducted using Design-Expert software 10.0, and the physical repose angle of fresh tea leaves was used as the response value to screen out the factors that had significant effects on the repose angle of machine-harvested fresh tea leaves. Each test parameter was set at two levels—that is, high (+1) and low (−1), denoted by X_1 to X_6. Based on the existing literature and a large number of simulation pre-tests, the value range of each simulation parameter was determined, as shown in Table 4, and a group of central point tests was added, totaling 13 test groups. The Plackett–Burman test protocol and results are shown in Table 5, and the analysis of variance (ANOVA) of the test results is shown in Table 6.

Table 4. Parameters of Plackett–Burman test.

Parameters	Symbol	Low Level (−1)	High Level (+1)
Tea leaves–tea leaves restitution coefficient	X_1	0.01	0.09
Tea leaves–tea leaves static friction coefficient	X_2	0.8	1.0
Tea leaves–tea leaves rolling friction coefficient	X_3	0.01	0.2
Tea leaves–PVC restitution coefficient	X_4	0.01	0.2
Tea leaves–PVC static friction coefficient	X_5	0.6	0.8
Tea leaves–PVC rolling friction coefficient	X_6	0.01	0.05

Table 5. Design and results of Plackett–Burman test.

Tests	X_1	X_2	X_3	X_4	X_5	X_6	Repose Angle (°)
1	1	1	−1	1	1	1	31.95
2	−1	1	1	−1	1	1	32.07
3	1	−1	1	1	−1	1	30.08
4	−1	1	−1	1	1	−1	30.96
5	−1	−1	1	−1	1	1	30.12
6	−1	−1	−1	1	−1	1	28.26
7	1	−1	−1	−1	1	−1	28.82
8	1	1	−1	−1	−1	1	29.74
9	1	1	1	−1	−1	−1	32.47
10	−1	1	1	1	−1	−1	31.51
11	1	−1	1	1	1	−1	31.48
12	−1	−1	−1	−1	−1	−1	28.45
13	0	0	0	0	0	0	31.76

Table 6. Analysis of significance of parameters in Plackett–Burman test.

Parameters	Standardization Effects	Sum of Squares	Contribution Rate/%	F Values	*p* Values
Model	—	22.16	—	13.02	0.0064 **
X_1	0.53	0.84	3.45	2.95	0.1464
X_2	1.92	11.00	45.33	38.79	0.0016 **
X_3	1.59	7.60	31.32	26.80	0.0035 **
X_4	0.43	0.55	2.27	1.94	0.2224
X_5	0.82	1.99	8.21	7.03	0.0454 *
X_6	−0.24	0.18	0.74	0.63	0.4617

Note: ** indicates extremely significant impact ($p < 0.01$), * indicates significant impact ($p < 0.05$). $R^2 = 0.8842$.

As is evident from Table 6, the model shows $p < 0.05$ and the coefficient of determination $R^2 = 0.8842$, indicating that the regression model is significant and can predict the trends of each parameter well. Moreover, $p < 0.01$ for X_2 (tea–tea static friction coefficient) and X_3 (tea–tea rolling friction coefficient), indicating that X_2 and X_3 have an extremely significant effect on the formation of the repose angle; $p < 0.05$ for X_5 (tea–PVC static friction coefficient), indicating that X_5 has a significant effect on the formation of the repose angle. By comparing the magnitude of the contribution of each parameter, the order of the effect of each parameter on the repose angle was X_2, X_3, X_5, X_1, X_4, and X_6.

In the subsequent steepest-ascent test and Box–Behnken test, only the three most significant parameters were considered. The standardized effects of X_2, X_3, and X_5 were all greater than 0, so their effects on the repose angle were positive. Consequently, in the subsequent steepest-ascent test, the factors that showed positive effects were gradually increased in fixed increments.

3.2. Analysis of the Steepest-Ascent Test Simulation Results

According to the significant parameters screened using the Plackett–Burman test, the parameters are increased or decreased in certain steps based on the degree of parameter influence: the parameters with less influence are taken up to the middle level of the values in Table 4 for the steepest-ascent test, and the relative error Y between the repose angle θ of the physical test and the repose angle θ' of the steepest-ascent test is calculated using Equation (5), so that the nearby area of the optimal value can be determined quickly. The calculation is as shown in Equation (5):

$$Y = \frac{|\theta' - \theta|}{\theta} \times 100\% \quad (5)$$

The design and results of the steepest-ascent test program are shown in Table 7, with the repose-angle relative error tending to decrease first before increasing, and the repose-angle relative error being the smallest under Test No. 3. Consequently, the parameters of Test No. 3 were used as the center point in the subsequent tests, and the parameters of Tests No. 2 and No. 4 were used as the low and high levels for response surface design, respectively.

Table 7. Design and results of steepest-ascent test.

Tests	X_2	X_3	X_5	Repose Angle (°)	Relative Error *Y*/%
1	0.80	0.01	0.60	31.21	4.32
2	0.85	0.05	0.65	32.26	1.10
3	0.90	0.10	0.70	32.87	0.77
4	0.95	0.15	0.75	33.32	2.15
5	1.00	0.20	0.80	35.42	8.58

3.3. Analysis of the Calibration Results of Fresh Tea Leaf Contact Parameters

Based on the results of the steepest-ascent test, the screened significant parameters were ranked, and three levels of low, medium, and high significant parameters were selected for the experimental design. The experimental parameter levels and codes were as shown in Table 8, and the experimental design scheme and results were as shown in Table 9, with the non-significant parameters all being taken up to the middle level.

Table 8. Significant parameter-level coding.

Level	X_2	X_3	X_5
−1	0.85	0.05	0.65
0	0.90	0.10	0.70
1	0.95	0.15	0.75

Table 9. Design and results of Box–Behnken test.

Tests	X_2	X_3	X_5	Repose Angle (°)
1	−1	−1	0	32.35
2	1	−1	0	32.98
3	−1	1	0	32.56
4	1	1	0	34.56
5	−1	0	−1	32.25
6	1	0	−1	33.25
7	−1	0	1	32.72
8	1	0	1	33.38
9	0	−1	−1	32.28
10	0	1	−1	32.45
11	0	−1	1	32.38
12	0	1	1	33.78
13	0	0	0	33.51
14	0	0	0	33.13
15	0	0	0	33.62
16	0	0	0	33.21
17	0	0	0	33.69

A multiple regression analysis of the experimental data using Design-Expert 10.0 software yielded a quadratic polynomial equation for the three significance parameters and the repose angle (θ), as shown in Equation (6):

$$\begin{aligned}\theta = 33.43 + 0.54X_2 + 0.42X_3 + 0.25X_5 + 0.34X_2X_3 - \\ 0.085X_2X_5 + 0.31X_3X_5 - 0.071X_2^2 - 0.25X_3^2 - 0.46X_5^2\end{aligned} \quad (6)$$

The results of the Box–Behnken test ANOVA are shown in Table 10. It is evident from the regression model that p = 0.0024, the lack of fit p = 0.4384 > 0.05, and the coefficient of determination R^2 = 0.9328; the regression model is highly significant, the lack of fit is not significant, the coefficient of determination is close to 1, and the coefficient of variation is 0.77%, indicating that the model is good and can predict the repose angle of fresh tea leaves well. As is evident from Table 10, X_2 (the tea–tea static friction coefficient), X_3 (the tea–tea rolling friction coefficient) and X_5^2 (the quadratic term of the static friction coefficient between tea and PVC) all have highly significant effects on the repose angle, and X_5 (the static friction coefficient between tea and PVC), X_2X_3 (the interaction term of the static friction coefficient between tea and the tea rolling friction coefficient) and X_3X_5 (the interaction term of the rolling friction coefficient between tea and the tea–PVC static friction coefficient) have significant effects on the repose angle. Among them, the response surfaces of the interaction terms between X_2, X_3 and X_5 for the repose angle are shown in Figure 10. As shown in Figure 10, the interaction effect between the two factors can be

visualized, and the graphs display a non-linear relationship between the repose angle and the factors. It can be seen that the effective surface curve of X_2 has a greater slope than X_3, which indicates that the contribution of X_2 to the repose angle is more significant than the X_3. Figure 10b shows the slope of X_3 surface curve is steeper than the X_5 direction, indicating that it has a more significant influence on the repose angle.

Table 10. Analysis of variance of Box–Behnken-test quadratic model.

Source of Variation	Sum of Squares	Freedom	Mean Square	F Value	*p* Value
Model	6.36	9	0.71	10.80	0.0024
X_2	2.30	1	2.30	35.14	0.0006
X_3	1.41	1	1.41	21.56	0.0024
X_5	0.52	1	0.52	7.87	0.0263
X_2X_3	0.47	1	0.47	7.17	0.0317
X_2X_5	0.029	1	0.029	0.44	0.5277
X_3X_5	0.38	1	0.38	5.78	0.0472
X_2^2	0.021	1	0.021	0.32	0.5869
X_3^2	0.26	1	0.26	3.97	0.0865
X_5^2	0.89	1	0.89	13.67	0.0077
Residual	0.46	7	0.065		
Lack of fit	0.21	3	0.070	1.13	0.4384
Pure error	0.25	4	0.062		
Sum	6.82	16			

R^2 = 0.9328; R^2_{adj} = 0.8465; CV = 0.77%; Adeq Precision = 12.160.

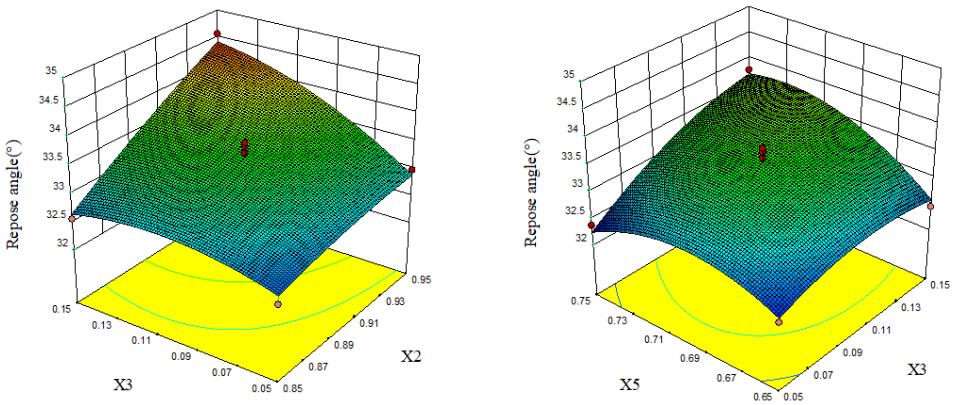

Figure 10. Effect of the interaction term on the repose angle: (**a**) interactive effects of X_2 and X_3; (**b**) interactive effects of X_3 and X_5.

3.4. Determination of Optimal Parameter Combinations and Experimental Verification

Using the optimization module in Design-Expert 10.0 software, the second-order regression equation (Equation (6)) could be optimally solved, using the physical test repose angle as the target value, and X_2, X_3, and X_5 as the optimization objects. According to Table 8, the values of X_2, X_3, and X_5 are 0.85–0.95, 0.05–0.15 and 0.65–0.75, respectively. Consequently, the objective function and constraint function of the optimization problem can be expressed, as shown in Equation (7):

$$\begin{cases} AOR(X_2, X_3, X_5) = 32.62^\circ \\ s.t. \begin{cases} 0.85 \le X_2 \le 0.95 \\ 0.05 \le X_3 \le 0.15 \\ 0.65 \le X_5 \le 0.75 \end{cases} \end{cases} \quad (7)$$

The optimal values of the three parameters are $X_2 = 0.865$, $X_3 = 0.067$, and $X_3 = 0.737$. To verify the accuracy of the optimal parameter combination, five repose-angle simulation tests were conducted with the above optimized parameter combinations as EDEM simulation parameters, the simulated repose angle measurements being 32.21°, 32.74°, 32.83°, 32.56°, and 32.33°, with an average value of 32.53° and a relative error of 0.28% with respect to the physical repose angle. The *t*-test was applied to analyze the simulated repose angle and the physical repose angle, and $p = 0.506 > 0.05$ was obtained, indicating that there was no significant difference between the simulated repose angle and the physical repose angle.

4. Conclusions

Using a 3D scanner and reverse engineering technology, a discrete element model of representative fresh tea leaves with different components was developed, which could provide a reference for DEM modeling of irregularly shaped crops. The intrinsic parameters of fresh tea leaves were measured using physical tests, and the Plackett–Burman test was conducted based on the simulation parameters obtained from physical tests and the related literature. The results were analyzed using ANOVA, and the parameters with a significant effect on the repose angle were obtained as the tea–tea static friction coefficient, the tea–tea rolling friction coefficient, and the static friction coefficient between tea and PVC, with the steepest-climb test being conducted to determine the range of significant parameters. Based on the Box–Behnken test results, a quadratic polynomial regression model of three significance parameters and a repose angle was determined, the repose angle of fresh tea leaves being used as the target value for the regression equation to find the optimal combination of the significance parameters; the best combination of the significance parameters was 0.865 for the static friction coefficient of tea leaves, 0.067 for the rolling friction coefficient of tea leaves, and 0.737 for the static friction coefficient between tea leaves and PVC. A *t*-test was then conducted and $p > 0.05$ was obtained, indicating that the simulation results were not significantly different from the physical test results, further verifying the reliability of the simulated parameter combinations. The results showed that the contact parameter calibration method for fresh tea leaves was feasible and could provide a basis for the discrete element study of machine-picked fresh tea leaf sorting and other work.

Author Contributions: R.W. and C.W.: conceptualization, methodology; D.L.: data curation, writing—original draft preparation; Y.Z.: analyzing, investigation; J.C.: writing, reviewing, and editing; G.Z.: writing, reviewing, and editing; C.W.: supervision. All authors have read and agreed to the published version of the manuscript.

Funding: This work was supported by the National Natural Science Foundation of China (grant numbers 52105283, 32301715 and 51975537), Major projects in Zhejiang Province (2023C02009), China Postdoctoral Science Foundation (Grant No.2022M722819) and Teacher Professional Development Project for Domestic Visiting Scholars in Universities (FX2022113).

Institutional Review Board Statement: Not applicable.

Data Availability Statement: The original contributions presented in the study are included in the article, further inquiries can be directed to the corresponding author/s.

Acknowledgments: The authors greatly appreciate the valuable comments and suggestions provided by the pre-publication reviewers.

Conflicts of Interest: The authors declare that they have no known competing financial interests or personal relationships that could have appeared to influence the work reported in this paper.

References

1. Mei, Y.; Zhang, S. Analysis of tea production and domestic sales situation in China in 2022. *China Tea* **2023**, *45*, 25–30.
2. Lu, H.W.; Wu, C.Y.; Tu, Z.; Chen, J.N.; Jia, J.M.; Chen, Z.W.; Ye, Y. Optimization of grading parameters of vibratory grader for fresh leaves of machine-picked tea based on EDEM. *Tea Sci.* **2022**, *42*, 120–130.

3. Zhang, J.; Xia, M.; Chen, W.; Yuan, D.; Wu, C.; Zhu, J. Simulation analysis and experiments for blade-soil-straw interaction under deep ploughing based on the discrete element method. *Agriculture* **2023**, *13*, 136. [CrossRef]
4. Weerasekara, N.S.; Powell, M.S.; Cleary, P.W.; Tavares, L.; Evertsson, M.; Morrison, R.; Quist, J.; de Carvalho, R. The contribution of DEM to the science of comminution. *Powder Technol.* **2013**, *248*, 3–24. [CrossRef]
5. Zheng, J.; Wang, L.; Wang, X.; Shi, Y.; Yang, Z. Parameter calibration of cabbages (*Brassica oleracea* L.) based on the discrete element method. *Agriculture* **2023**, *13*, 555. [CrossRef]
6. Horabik, J.; Molenda, M. Parameters and contact models for DEM simulations of agricultural granular materials: A review. *Biosyst. Eng.* **2016**, *147*, 206–225. [CrossRef]
7. Rackl, M.; Hanley, K.J. A methodical calibration procedure for discrete element models. *Powder Technol.* **2017**, *307*, 73–83. [CrossRef]
8. Marczewska, I.; Rojek, J.; Kačianauskas, R. Investigation of the effective elastic parameters in the discrete element model of granular material by the triaxial compression test. *Arch. Civ. Mech. Eng.* **2016**, *16*, 64–75. [CrossRef]
9. Qiu, Y.; Guo, Z.; Jin, X.; Zhang, P.; Si, S.; Guo, F. Calibration and verification test of cinnamon soil simulation parameters based on discrete element method. *Agriculture* **2022**, *12*, 1082. [CrossRef]
10. Hou, Z.F.; Dai, N.Z.; Chen, Z.; Chou, Y.; Zhang, X.W. Determination and evaluation of physical parameters of Wheatgrass seeds leave calibration of discrete element simulation parameters. *Trans. CSAE* **2020**, *36*, 46–54. (In Chinese)
11. Wang, Y.; Zhang, Y.; Yang, Y.; Zhao, H.; Yang, C.; He, Y.; Xu, H. Discrete element modelling of citrus fruit stalks and its verification. *Biosyst. Eng.* **2020**, *200*, 400–414. [CrossRef]
12. Liao, Y.; Liao, Q.; Zhou, Y.; Wang, Z.; Jiang, Y.; Liang, F. Parameters calibration of discrete element model of fodder rape crop harvest in bolting stage. *Trans. CSAE* **2020**, *51*, 73–82.
13. Kattenstroth, R.; Harms, H.H.; Lang, T. Systematic alignment of straw to optimise the cutting process in a combine's straw chopper. In Proceedings of the 69th International Conference on Agricultural Engineering Land Technik AgEng, Hannover, Germany, 11–12 November 2011.
14. Fang, M.; Yu, Z.; Zhang, W.; Cao, J.; Liu, W. Friction coefficient calibration of corn stalk particle mixtures using Plackett–Burman design and response surface methodology. *Powder Technol.* **2022**, *396*, 731–742. [CrossRef]
15. Liu, F.; Zhang, J.; Chen, J. Modeling of flexible wheat straw by discrete element method and its parameter calibration. *Int. J. Agric. Biol. Eng.* **2018**, *11*, 42–46. [CrossRef]
16. Lenaerts, B.; Aertsen, T.; Tijskens, E.; De Ketelaere, B.; Ramon, H.; De Baerdemaeker, J.; Saeys, W. Simulation of grain–straw separation by discrete element modeling with bendable straw particles. *Comput. Electron. Agric.* **2014**, *101*, 24–33. [CrossRef]
17. Du, C.; Han, D.; Song, Z.; Chen, Y.; Chen, X.; Wang, X. Calibration of contact parameters for complex shaped fruits based on discrete element method: The case of pod pepper (*Capsicum annuum*). *Biosyst. Eng.* **2023**, *226*, 43–54. [CrossRef]
18. Fan, G.; Wang, S.; Shi, W.; Gong, Z.; Gao, M. Simulation parameter calibration and test of typical pear varieties based on discrete element method. *Agronomy* **2022**, *12*, 1720. [CrossRef]
19. Ren, J.H.; Wu, T.; Mo, W.Y.J.; Li, K.; Hu, P.; Xu, F.Y.; Liu, Q.T. Discrete element simulation modeling method and parameters calibration of sugarcane leaves. *Agronomy* **2022**, *12*, 1796. [CrossRef]
20. Zhu, J.; Zou, M.; Liu, Y.; Gao, K.; Su, B.; Qi, Y. Measurement and calibration of DEM parameters of lunar soil simulant. *Acta Astronaut.* **2022**, *191*, 169–177. [CrossRef]
21. Zhang, S.; Yang, F.; Dong, J.; Chen, X.; Liu, Y.; Mi, G.; Wang, T.; Jia, X.; Huang, Y.; Wang, X. Calibration of discrete element parameters of maize root and its mixture with soil. *Processes* **2022**, *10*, 2433. [CrossRef]
22. Yu, Y.; Ren, S.; Li, J.; Chang, J.; Yu, S.; Sun, C.; Chen, T. Calibration and testing of discrete element modeling parameters for fresh Goji berries. *Appl. Sci.* **2022**, *12*, 11629. [CrossRef]
23. Gou, F.Q.; Yi, Z.H.; Niu, X.W.; Yan, I.B. Discrete element parameter calibration of edible rose petals based on virtual stacking test. *Food Mach.* **2022**, *38*, 106–110+130.
24. Sun, X.; Li, B.; Liu, Y.; Gao, X. Parameter measurement of edible sunflower exudates and calibration of discrete element simulation parameters. *Processes* **2022**, *10*, 185. [CrossRef]
25. Liu, M.; Hou, Z.F.; Ma, X.J.; Dai, N.Z.; Zhang, X.W. Discrete element-based calibration and testing of alfalfa seed simulation parameters. *Jiangsu Agric. Sci.* **2022**, *50*, 168–175.
26. Han, D.-D.; Xu, Y.; Huang, Y.-X.; He, B.; Dai, J.-W.; Lv, X.-R.; Zhang, L.-H. DEM parameters calibration and verification for coated maize particles. *Comput. Part. Mech.* **2023**, *10*, 1931–1941. [CrossRef]
27. Xie, Z.B.; Yi, Z.H.; Niu, X.W.; Yao, Z. Analysis of petal throwing motion trajectory in petal color sorter. *Softw. Guide* **2020**, *19*, 117–121.
28. Li, B.; Li, W.N.; Xuan, B.B.; Zhang, Z.Z. Study on the sieving rate of tea fresh leaf classifier based on EDEM. *Tea Sci.* **2019**, *39*, 484–494.
29. Xia, R.; Li, B.; Wang, X.; Li, T.; Yang, Z. Measurement and calibration of the discrete element parameters of wet bulk coal. *Measurement* **2019**, *142*, 84–95. [CrossRef]